Nonlinear Stochastic Dynamics of an Energy Harvester with Matched Load

NONLINEAR STOCHASTIC DYNAMICS OF AN ENERGY HARVESTER WITH MATCHED LOAD

Kailing Song[1,2,*[0000-0003-0564-3905]] and Michele Bonnin[2[0000-0002-9106-563X]]

[1] IUSS Pavia, Palazzo del Broletto, Piazza della Vittoria, 15, 27100 Pavia, Italy
[2] Politecnico di Torino, Corso Duca degli Abruzzi, 24, 10129 Torino, Italy
*kailing.song@polito.it

Abstract. Nonlinear energy harvesting is a promising technology to supply power or recharge batteries, to micro-electromechanical-systems requiring small amount of energy for their operation. Nonlinear response and multi-stability, can be exploited to increase the energy scavenged and the power efficiency of energy harvesting systems. In this work, we analyze the dynamics of a nonlinear, bi-stable energy harvester subject to random mechanical vibrations. As a solution to further increase the harvested power, we propose the application of an impedance matching network. The role of the matching network is to optimize the energy transfer from an oscillating mechanism, designed to capture vibration kinetic energy, to the electrical load. The systems is described by a set of nonlinear stochastic differential equation. We use a power series expansion method to find an approximate solution of the stochastic differential equations, in the weak noise limit. The approximate solution is the used to optimize the circuit parameters of the impedance matching network. In the strong noise limit, the state equations are integrated numerically to determine average power absorbed by the load and power efficiency. Our analysis shows that the application of the optimized matching network improves the performances by a significant amount with respect to a direct connection of the load.

Keywords: Renewable energy, sustainable energy, energy harvesting, stochastic differential equations, power series method, stochastic processes, impedance matching.

1 Introduction

Energy harvesting is a fast growing research area, that promise to realize electromechanical systems capable of self-powering, or that could at least recharge their internal batteries, scavenging energy dispersed in the surrounding environment. As such, energy harvesting represents a particularly promising solution for powering a wide range of applications, in particular those belonging to the Internet of Things, that are characterized by low power consumption, miniaturization and wireless connections [1].

Depending on the application under exam, different ambient energy sources can be exploited. In the case of miniaturized systems that require small amount of energy, very promising sources are dispersed electromagnetic waves, small thermal gradients, and

even human motion [2, 3, 4, 5, 6]. Ambient mechanical vibrations are promising [2], because they are ubiquitous, they are characterized by a relatively high power density, and they can be easily converted into usable electrical power, exploiting different physical transduction mechanisms [7].

One of the main challenges in the design of energy harvesting systems is the sub-optimal energy transfer from the mechanical structure to the electrical load, as a consequence of the large impedance mismatch between the two different domains. In fact, mechanical and electrical systems are characterized by time scales (time constant and/or resonant frequencies) that may differ by several order of magnitude. Impedance mismatch is a classical problem in electronic engineering, in particular in RF applications. The classical approach to cope with this class of problems is impedance matching. Impedance matching consists in interposing a properly designed matching network between the harvester and the load to eliminate the mismatch [8, 9, 10].

To keep the problem more tractable, ambient vibrations are often modelled by a simple periodic function, e.g. a sinusoid. Such an approximation is reasonable when the energy of ambient vibrations is concentrated at a single frequency. The main advantage of using a single sinusoid approximation is that the theory of periodically driven nonlinear oscillators is well developed, and sophisticated method of analysis are available [8]. However, in most practical cases the energy of ambient vibrations is distributed over a relatively wide frequency interval, and a sinusoidal approximation is not justified. Instead, if a more realistic description is represented by a stochastic process. In particular, for vanishingly small correlation time, ambient vibrations can be conveniently modeled as a white Gaussian noise forcing term.

In this work, we consider the mathematical model of a bi-stable energy harvester with a piezoelectric transducer, subject to random mechanical vibrations modelled as white Gaussian noise. We use both analytical and numerical methods to analyze the dynamic behavior of the energy harvester. The mathematical model of the energy harvester is obtained from the Lagrange equation of motion for the mechanical part, and from the circuit description of the electrical load. The piezoelectric transducer is assumed to be linear.

The energy harvester design includes nonlinearities in the elastic force, thanks to a special arrangement of magnets. Consequently, the governing equations are nonlinear stochastic differential equations (SDEs) that do not admit for an analytical solution. Instead, we use a power series method to obtain an approximate solution in the weak noise limit, and numerical integration in the strong noise limit. To improve the efficiency and the scavenged power, we apply a solution inspired by circuit theory, and in particular RF applications, that we have recently applied to mono-stable energy harvesters. The solution consists of introducing a matching network between the energy harvester and the load [8, 10]. We use the approximate solution obtained trough the power series method to optimize the matching network, and we evaluate the advantage offered by the matching network in terms of output average voltage, average harvested power and total power efficiency.

2 Modelling

A typical cantilever beam energy harvester for ambient mechanical vibration, with piezoelectric transducer is exemplified in figure 1. The harvester is composed of the beam, fixed at the lower end to a vibrating support. Vibrations of the support produce oscillations of the beam, that are amplified by an inertial mass *m* fixed at the upper end of the beam. The oscillations produce mechanical stress in a layer of piezoelectric material covering the beam, which are converted into electrical power.

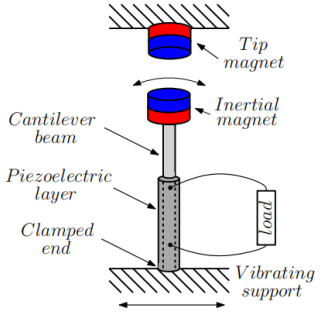

Fig. 1. Exemplification of a cantilever beam, bi-stable energy harvester with piezoelectric transducer.

In this setup the inertial mass is a magnet. A nonlinear elastic force is obtained introducing a tip magnet, that is fixed to a support in front in the inertial magnet with opposed polarities, creating a biased inverted pendulum with a magnetic repulsive force. If the two magnets are very close, the magnetic repulsion forces the beam either to the left or to the right of the vertical position. In the absence of ambient vibrations, the beam exhibits bi-stability. Three stable resting positions exist: the vertical position, that is unstable, plus the two stable resting positions.

The governing equations can be derived from classical mechanics, the characterization of piezoelectric materials, and the circuit description of the electrical load [8, 10]. For the mechanical part and the piezoelectric transducer we have:

$$m\,\ddot{x} + \gamma\,\dot{x} + U'(x) + \alpha\,e = f_{ext}(t) \tag{1a}$$

$$C_{pz}\,\dot{e} + \alpha\,\dot{x} + I_{load} = 0 \tag{1b}$$

where x is the displacement of the inertial mass m from the vertical position, γ is the internal camping constant, α is the electro-mechanical coupling constant (measured in N/V or As/m), C_{pz} and e are the electrical capacitance and the voltage across the piezoelectric transducer, respectively. Finally, I_{load} is the current relative to the electrical load. $U(x)$ represents the elastic potential of the beam, and we shall assume $U(x) = -k_1 x^2/2 + k_3 x^4/4$ to account for the bi-stability. $f_{ext}(t)$ is the external force due to the vibrating support, that will be modeled as white Gaussian noise

For the electrical load, we shall consider two scenarios. The load is typically modeled as resistor, see figure 3(a). In this case, application of Ohm's law gives $I_{load} = G_L$

e, where $G_L = R_L^{-1}$ is the load conductance. However, resistors cannot match the reactive component of the harvester impedance, unless the latter is working exactly at the resonant frequency. A solution consists in introducing a matching network, as the one shown in figure 3(b), between the harvester and the load. The matching network includes only reactive elements (inductors and capacitors, as in the example of Fig. (b)), because reactive elements do not absorb average power, but rather decrease the impedance mismatch between the source and the load, reducing the reactive power that flows back and forth, and thus improving the power efficiency of the harvester.

To illustrate the role of the matching network, consider a periodically forced linear circuit, as the one shown in figure 2. The circuit is composed by a linear two terminal element with impedance $Z_G = R_G + jX_G$, where $j = \sqrt{-1}$, and R_G, X_G are the element's resistance and reactance, respectively, two reactive elements with reactance X_S and X_P, respectively, and a resistor with resistance *R*.

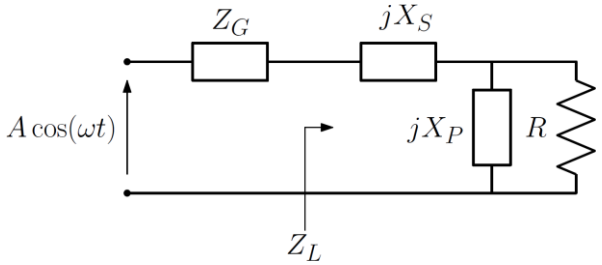

Fig. 2 Periodically driven linear circuit with a LC matching network.

According to the maximum power transfer theorem, the resistor *R* absorbs maximum average power if, and only if, the impedance Z_L, as shown in the figure, is the complex conjugate of Z_G, that is $Z_L = R_G - jX_G$. It is straightforward finding:

$$Z_L = jX_S + \frac{jR^2X_P + R\,X_P^2}{R^2 + X_P^2}$$

It follows that the reactive elements in the matching networks must satisfy (assuming $R > R_G$): $X_P^2 = \frac{R_G R^2}{R - R_G}$; $X_S = -X_G - \frac{R^2 X_P}{R^2 + X_P^2}$.

The last two equations show that, if the linear system is working at the resonant frequency, and the load resistance is equal to the source resistance ($X_G = 0\ \Omega$ and $R = R_G, respectively$), then the shunted element in parallel with the resistor must behave as an open circuit with $X_P \to +\infty$, while the element connected in series must behave as a short circuit with $X_S = 0\ \Omega$. However, the two aforementioned conditions are rarely met in energy harvesting applications. In fact, even in the case where mechanical energy is mostly concentrated at one frequency, this frequency may change in time. Moreover, the load resistance will in most case be fixed and cannot match the harvester resistance. Therefore, in the most general case where $R \neq R_G$, and $X_G \neq 0\ \Omega$, two reactive elements are necessary to match both the source resistance and reactance.

Clearly, a perfect matching is possible only at a single frequency, whereas in energy harvesting applications the energy of ambient vibrations is in general distributed over a wide frequency interval. The problem is also made more difficult because the energy

harvester is a nonlinear system. Nevertheless, our analysis shows that it is possible to design a matching network that achieves partial matching over a relative wide frequency band, thus maximizing the harvested power and the power efficiency.

For the matched load scenario, application of Kirchhoff current and voltage laws gives $I_{load} = C_P\dot{v}_0 + G_L v_0$ and $L_s\dot{I}_{load} = v_0 - e$.

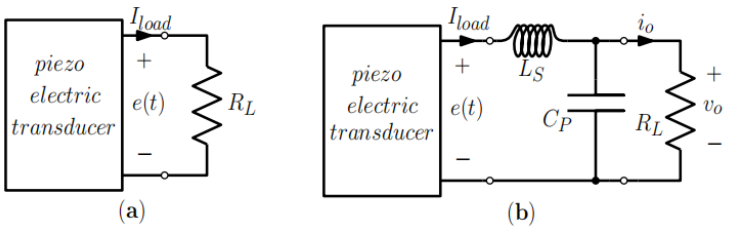

Fig. 3. **(a)** Resistive load. **(b)** Example of application of a matching network: Resistive load with low-pass LC matching network.

Combining (1) together with the equations for the electrical part, and rewriting the differential equations as a system of first order Itô SDEs, we obtain for the resistive load

$$dx = ydt \tag{2a}$$

$$dy = (-\frac{1}{m}U'(x) - \frac{\gamma}{m}y - \frac{\alpha}{m}e)dt + \frac{\varepsilon}{m}dW_t \tag{2b}$$

$$de = (\frac{\alpha}{C_{pz}}y - \frac{G_L}{C_{pz}}e)dt \tag{2c}$$

where ε is a positive parameter that defines the noise intensity. Analogously, For the matched load we find

$$dx = ydt \tag{3a}$$

$$dy = (\frac{1}{m}U'(x) - \frac{\gamma}{m}y - \frac{\alpha}{m}e)dt + \frac{\varepsilon}{m}dW_t \tag{3b}$$

$$de = (\frac{\alpha}{C_{pz}}y + \frac{1}{C_{pz}}I)dt \tag{3c}$$

$$dI = (\frac{1}{L_s}v_0 - \frac{1}{L_s}e)dt \tag{3d}$$

$$dv_0 = (-\frac{1}{C_P}I - \frac{G_L}{C_P}v_0)dt \tag{3e}$$

being W_t the one-dimensional Wiener process.

3 Analysis

Finding the matching network circuit parameters' that maximize the harvested power, requires to solve the SDEs (3), or at least to find the first two moments of the probability distribution for the output voltage v_o. Obtaining the exact solution of nonlinear SDEs is, in general, unfeasible, while finding the moments require long simulations, that must be repeated for all parameter values, thus making also this approach unpractical.

Here we tackle the problem differently. We apply a perturbation method to find an approximate solution for the SDEs in the limit of small noise intensity. This approximated solution is then used to determine the circuit parameters that maximize the harvested power.

Consider a d-dimensional system of SDEs with a one-dimensional Wiener process W_t

$$d\boldsymbol{X}_t = \boldsymbol{a}(\boldsymbol{X}_t)dt + \varepsilon\, \boldsymbol{B}(\boldsymbol{X}_t)dW_t \tag{4}$$

For small values of ε, we look for a solution in the form of a power series of the same small parameter

$$\boldsymbol{X}_t = \boldsymbol{X}_0 + \varepsilon\, \boldsymbol{X}_1 + \varepsilon^2 \boldsymbol{X}_2 + \ldots \tag{5}$$

In the same way, we expand the drift vector in Taylor series as (notice that subscript t denoting time dependence is dropped in $\boldsymbol{X}_k$, k = 0, 1, 2,… for the sake of notation simplicity)

$$\boldsymbol{a}(\boldsymbol{X}) = \boldsymbol{a}(\boldsymbol{X}_0) + \boldsymbol{A}_1(\boldsymbol{X}_0)(\varepsilon \boldsymbol{X}_1 + \varepsilon^2 \boldsymbol{X}_2) + \boldsymbol{A}_2(\boldsymbol{X}_0, \boldsymbol{X}_1) + \boldsymbol{O}(\varepsilon^3) \tag{6}$$

where $\boldsymbol{A}_1(\boldsymbol{X}_0) = \left.\partial \boldsymbol{a}/\partial \boldsymbol{x}\right|_{\boldsymbol{X}_0}$ denotes the Jacobian matrix of $\boldsymbol{a}$, and $\boldsymbol{A}_2(\boldsymbol{X}_0, \boldsymbol{X}_1)$ is the vector with components

$$\boldsymbol{A}_{2,\boldsymbol{i}}(\boldsymbol{X}_0, \varepsilon^2 \boldsymbol{X}_1) = \frac{1}{2} \varepsilon^2 \boldsymbol{X}_1^T \boldsymbol{H}_{\boldsymbol{i}}(\boldsymbol{X}_0) \boldsymbol{X}_1 \tag{7}$$

Being $\boldsymbol{H}_i$ the Hessian matrix $\boldsymbol{H}_i(\boldsymbol{X}_0) = \left.\partial^2 a_i \big/ \partial x^2\right|_{\boldsymbol{X}_0}$.

Finally, we take the Taylor expansion of the diffusion vector:

$$\boldsymbol{B}(\boldsymbol{X}) = \boldsymbol{B}(\boldsymbol{X}_0) + \boldsymbol{B}_1(\boldsymbol{X}_0)(\varepsilon \boldsymbol{X}_1 + \varepsilon^2 \boldsymbol{X}_2) + \boldsymbol{O}(\varepsilon^2) \tag{8}$$

where $\boldsymbol{B}_1(\boldsymbol{X}_0) = \left.\partial \boldsymbol{B} \big/ \partial \boldsymbol{x}\right|_{\boldsymbol{X}_0}$.

Substituting (5), (6) and (8) into (4), and equating the terms of the same powers of ε, gives the system of equations:

$$\varepsilon_0 : \quad d\boldsymbol{X}_0 = a(\boldsymbol{X}_0)dt \tag{9a}$$

$$\varepsilon_1 : \quad d\boldsymbol{X}_1 = \boldsymbol{A}_1(\boldsymbol{X}_0)\boldsymbol{X}_1 dt + \boldsymbol{B}(\boldsymbol{X}_0)dW_t \tag{9b}$$

$$\varepsilon_2: \qquad d\boldsymbol{X}_2 = (\boldsymbol{A}_1(\boldsymbol{X}_0)\boldsymbol{X}_2 + \boldsymbol{A}_2(\boldsymbol{X}_0, \boldsymbol{X}_1))dt + \boldsymbol{B}_1(\boldsymbol{X}_0)\boldsymbol{X}_1 dW_t \tag{9c}$$

Equations (9) form a system of differential equations, which requires a a set of appropriate initial conditions so that the solutions $\boldsymbol{X}_0(t)$, $\boldsymbol{X}_1(t)$, and $\boldsymbol{X}_2(t)$ become unique. Without loss of generality we assume: $\boldsymbol{X}_0(0) = \boldsymbol{x}_0$, $\boldsymbol{X}_1(0) = \boldsymbol{X}_2(0) = 0$.

The order zero equation (9a), is a nonlinear, ordinary differential equation (ODE) describing the "underlying" deterministic problem. Again, without loss of generality, the initial condition is chosen such that $\boldsymbol{x}_0$ corresponds to an asymptotically stable equilibrium point, implying that the solution is $\boldsymbol{X}_0(t) = \boldsymbol{x}_0$ for all t. The order one SDE (9b) implies that $\boldsymbol{X}_1(t)$ is an Ornstein-Uhlenbeck process [11, 12], that can be calculated analytically. Finally, the order two SDE (9c) describes a linear system of non-homogeneous SDEs. The process can be iterated to include higher order terms, obtaining equations that become increasingly complicated.

4 Moments calculation

Taking expectations in (5), the following expression for the first order moment of the solution is obtained: $\langle \boldsymbol{X}_t \rangle = \boldsymbol{X}_0 + \varepsilon \langle \boldsymbol{X}_1 \rangle + \varepsilon^2 \langle \boldsymbol{X}_2 \rangle + \boldsymbol{O}(\varepsilon^3)$.

Concerning second order moments, using again (5) we find

$$\begin{aligned} \boldsymbol{X}_t \boldsymbol{X}_t^{\boldsymbol{T}} &= \boldsymbol{X}_0 \boldsymbol{X}_0^{\boldsymbol{T}} + \varepsilon(\boldsymbol{X}_0 \boldsymbol{X}_1^{\boldsymbol{T}} + \boldsymbol{X}_1 \boldsymbol{X}_0^{\boldsymbol{T}}) \\ &\quad + \varepsilon^2(\boldsymbol{X}_0 \boldsymbol{X}_2^{\boldsymbol{T}} + \boldsymbol{X}_1 \boldsymbol{X}_1^{\boldsymbol{T}} + \boldsymbol{X}_2 \boldsymbol{X}_0^{\boldsymbol{T}}) + \boldsymbol{O}(\varepsilon^3) \end{aligned} \tag{10}$$

Taking expectation:

$$\begin{aligned} \langle \boldsymbol{X}_t \boldsymbol{X}_t^{\boldsymbol{T}} \rangle &= \boldsymbol{X}_0 \boldsymbol{X}_0^{\boldsymbol{T}} + \varepsilon(\boldsymbol{X}_0 \langle \boldsymbol{X}_1^{\boldsymbol{T}} \rangle + \langle \boldsymbol{X}_1 \rangle \boldsymbol{X}_0^{\boldsymbol{T}}) \\ &\quad + \varepsilon^2(\boldsymbol{X}_0 \langle \boldsymbol{X}_2^{\boldsymbol{T}} \rangle + \langle \boldsymbol{X}_1 \boldsymbol{X}_1^{\boldsymbol{T}} \rangle + \langle \boldsymbol{X}_2 \rangle \boldsymbol{X}_0^{\boldsymbol{T}}) + \boldsymbol{O}(\varepsilon^3) \end{aligned} \tag{11}$$

Therefore, all moments are calculated as linear combinations of the first order moments $\langle \boldsymbol{X}_1 \rangle, \langle \boldsymbol{X}_2 \rangle$, and of the second order moments $\langle \boldsymbol{X}_1 \boldsymbol{X}_1^{\boldsymbol{T}} \rangle$.

Taking stochastic expectations on both sides of (9), and using the martingale property of Itô integrals gives:

$$\frac{d}{dt}\langle \boldsymbol{X}_1 \rangle = \boldsymbol{A}_1(\boldsymbol{X}_0)\langle \boldsymbol{X}_1 \rangle \tag{12a}$$

$$\frac{d}{dt}\langle \boldsymbol{X}_2 \rangle = \boldsymbol{A}_1(\boldsymbol{X}_0)\langle \boldsymbol{X}_2 \rangle + \langle \boldsymbol{A}_2(\boldsymbol{X}_0, \boldsymbol{X}_1) \rangle \tag{12b}$$

The asymptotic stability hypothesis implies that all the eigenvalues of $\boldsymbol{A}_1(\boldsymbol{X}_0)= \partial \boldsymbol{a} / \partial \boldsymbol{x}|_{\boldsymbol{X}_0}$ have negative real parts, and therefore $\langle \boldsymbol{X}_1 \rangle \to 0$ as $t \to 0$. For $\langle \boldsymbol{X}_2 \rangle$, we have at steady state

$$\langle \boldsymbol{X}_2 \rangle = -\boldsymbol{A}_1^{-1}(\boldsymbol{X}_0)\langle \boldsymbol{A}_2(\boldsymbol{X}_0, \boldsymbol{X}_1) \rangle \tag{13}$$

To calculate $\langle \boldsymbol{A}_2(\boldsymbol{X}_0, \boldsymbol{X}_1) \rangle$ we need $\langle \boldsymbol{X}_1^T \boldsymbol{H}_i(\boldsymbol{X}_0) \boldsymbol{X}_1 \rangle$. Taking into account that asymptotically $\langle \boldsymbol{X}_1 \rangle = 0$, that matrices $\boldsymbol{H}_i(\boldsymbol{X}_0)$ are symmetric, and using the cyclic property of the trace, we find

$$\left\langle \boldsymbol{X}_1^T \boldsymbol{H}_i(\boldsymbol{X}_0) \boldsymbol{X}_1 \right\rangle = tr(\boldsymbol{H}_i(\boldsymbol{X}_0) \sigma_{\boldsymbol{X}_1 \boldsymbol{X}_1}) \tag{14}$$

Where $\sigma_{\boldsymbol{X}_1 \boldsymbol{X}_1} = \left\langle \boldsymbol{X}_1 \boldsymbol{X}_1^T \right\rangle$ is the covariance matrix of $\boldsymbol{X}_1$.

The covariance matrix is calculated as follows: Using Itô calculus (we write $\boldsymbol{B}_0 = \boldsymbol{B}(\boldsymbol{X}_0)$ and $\boldsymbol{A}_1$ instead of $\boldsymbol{A}_1(\boldsymbol{X}_0)$ for simplicity of notation) we find

$$d(\boldsymbol{X}_1 \boldsymbol{X}_1^T) = (\boldsymbol{A}_1 \boldsymbol{X}_1 \boldsymbol{X}_1^T + \boldsymbol{X}_1 \boldsymbol{X}_1^T \boldsymbol{A}_1^T + \boldsymbol{B}_0 \boldsymbol{B}_0^T) dt + (\boldsymbol{B}_0 \boldsymbol{X}_1^T + \boldsymbol{X}_1 \boldsymbol{B}_0^T) dW_t \tag{15}$$

Taking stochastic expectations and using again the martingale property we obtain the Lyapunov equation:

$$\frac{d}{dt} \sigma_{\boldsymbol{X}_1 \boldsymbol{X}_1} = \boldsymbol{A}_1 \sigma_{\boldsymbol{X}_1 \boldsymbol{X}_1} + \sigma_{\boldsymbol{X}_1 \boldsymbol{X}_1} \boldsymbol{A}_1^T + \boldsymbol{B}_0 \boldsymbol{B}_0^T \tag{16}$$

The steady state solution yields the algebraic equation for the covariance matrix

$$\boldsymbol{A}_1 \sigma_{\boldsymbol{X}_1 \boldsymbol{X}_1} + \sigma_{\boldsymbol{X}_1 \boldsymbol{X}_1} \boldsymbol{A}_1^T + \boldsymbol{B}_0 \boldsymbol{B}_0^T = 0 \tag{17}$$

Note that because $\boldsymbol{A}_1$ is stable and $\boldsymbol{B}_0 \boldsymbol{B}_0^T$ is symmetric, the covariance matrix solution of the Lyapunov equation is unique.

5 Results and discussion

We applied the previous technique to the piezoelectric cantilever beam energy harvester described in section 2. The parameter values are taken from [8, 10, 13]. To account for bi-stability, we have assumed that the elastic potential is: $U(x) = -k_1 x^2/2 + k_3 x^4/4$. Consequently, the harvester has three equilibrium points. The origin is an unstable equilibrium of saddle type, while the equilibria,

$$\pm \boldsymbol{x}_0^T = [\bar{x}, \bar{y}, \bar{e}, \bar{\imath}, \bar{v}_0] = [\pm\sqrt{k_1/k_3}, 0,0,0,0]$$

which are stable of focus type.

The average power absorbed by the load is proportional to the root mean square value of the output voltage: $P_L = G_L v_{0(rms)} = G_L \sqrt{\langle v_0^2(t) \rangle}$. We applied the

methodology described in sections 3 and 4 to calculate the expected quantity $\langle \boldsymbol{X}_t \boldsymbol{X}_t^T \rangle$ given by (11), for each value of the matching network parameters L_S and C_P within a certain range. The optimum values of L_S and C_P that maximize the last component of $\langle \boldsymbol{X}_t \boldsymbol{X}_t^T \rangle$ (such component corresponds to the square of $v_o(rms)$) where thus found without the need to solve the SDEs (3). In the analysis, ambient vibrations were modeled using mechanical to electrical analogies, making use of a white Gaussian noise voltage source with intensity ε = 200 mV.

Figure 3 shows the root mean square of the output voltage versus the parameters of the matching network L_S and C_P. There is a wide set of parameters' values that maximize the output voltage. It is worth mentioning that the very high values of the inductance L_S (and of the root mean square output voltage) are due to the normalization imposed on the harvester mechanical parameters, as discussed in [10, 13].

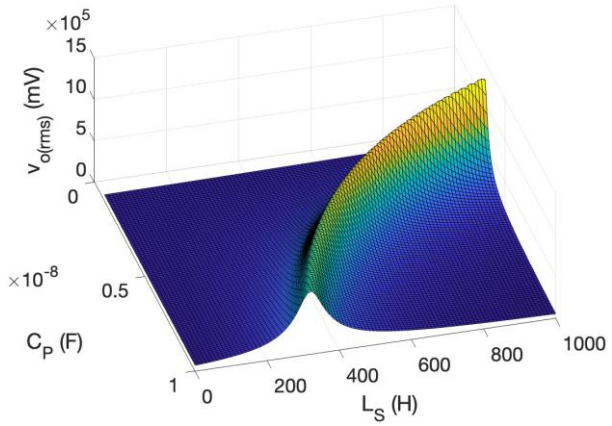

Fig. 4. Result of matching network optimization: Root mean square value of the output voltage $\sqrt{\langle v_0^2(t) \rangle}$ as a function of the parameters of the matching network L_S and C_P.

We used the approximated solution obtained through the power series method for the optimization of the matching network. The optimization gives a good result for small values of the noise intensity. To verify whether the matching network offers significant advantages also for intermediate and large values of the parameter ε, we have integrated numerically the SDEs (2) and (3) for large ε, and we have calculated average output voltage from the numerical solution. The numerical integration has been performed using different numerical integration schemes. In particular we used both the Euler-Maruyama and the stochastic Runge-Kutta methods [14]. For both numerical methods, the integration length of each simulation was set to $\Delta t = 10^4$s, and the integration step was $\delta t \backsim 30$ μs. Because the integration step was relatively small, we have not observed significant differences between the two numerical schemes. For more

accurate results, we run 20 simulations, each one with a different realizations of the Wiener process, for each set of parameters' values, and we averaged the results after eliminating the transient portion of the solution.

Figures 4 and 5 show the displacement $x(t)$ versus time, obtained through numerical simulations, for the energy harvester with resistive and with the matching network, respectively. On the left, it is shown the displacement for ε = 200 mV. On the right, it is shown the displacement for ε = 500 mV. For small amplitude vibrations the cantilever beam remains confined to the neighborhood of the stable equilibrium point (which one is determined by the initial condition), while for relatively large intensity the mass jumps from the basin of attraction of one equilibrium point to the other occur. The jumps occur at random time instants.

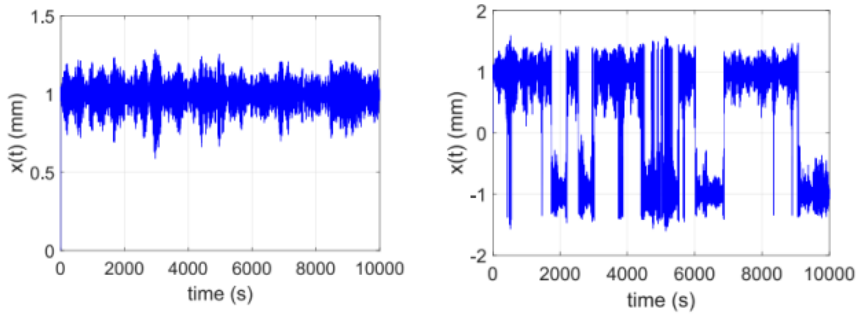

Fig. 5. Position $x(t)$ versus time for the energy harvester with the resistive load. Left: small noise intensity ε = 200mV. Right: large noise intensity ε = 500m. Null initial conditions.

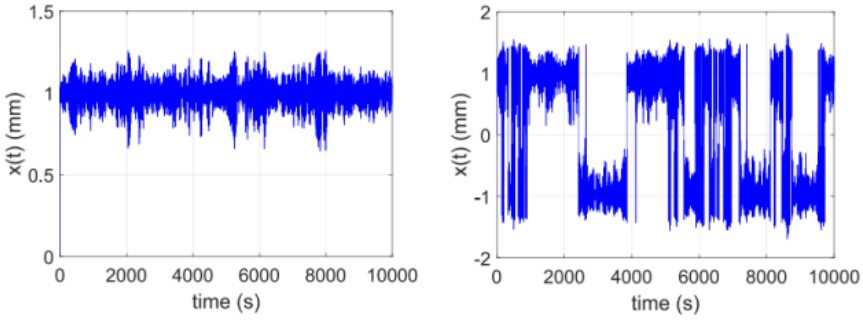

Fig. 6. Position $x(t)$ versus time for the energy harvester with matching network. Left: small noise intensity ε = 200mV. Right: large noise intensity ε = 500mV. Null initial conditions.

Finally, figure 6 shows the root mean square output voltage as a function of ε. The root mean square output voltage for the harvester with simple resistive load is compared to the case of the harvester with matched load. Application of the matched load increases the output voltage by more than three times for practically all vibration

intensities. Consequently, the average output power provided by the energy harvester with matched load increases by more than nine times.

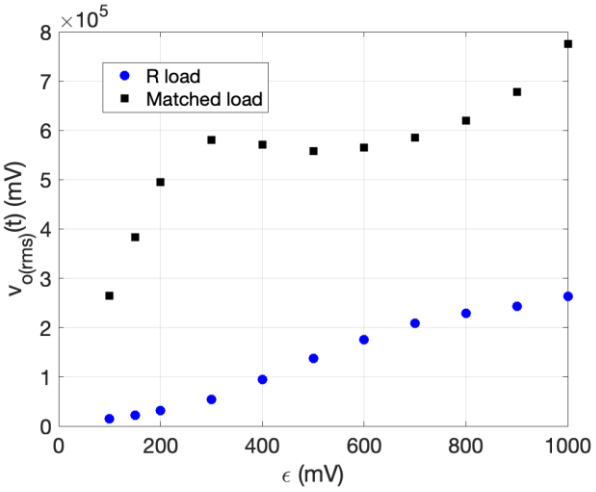

Fig. 7. Comparison of the root mean square of the output voltage versus vibration intensity for the harvester with resistive and with matched load.

6 Conclusions

Energy harvesting is a promising solution for the realization of miniaturized electro-mechanical system capable of self-powering, or at least capable of recharging their interval batteries, by scavenging power from the external environment. Such a technical solution is particularly well suited for low power Internet of Things applications.

This paper is devoted to the modelling and analysis of a bi-stable energy harvester for ambient mechanical vibrations, with a piezoelectric transducer. The mathematical model is derived from the Lagrange equation of motion of a mechanical oscillator, and a circuit description of the electrical load. The piezoelectric transducer is assumed to be linear. We consider the inclusion of a matching network between the energy harvester and the electrical load.

We assume that the restoring elastic force for the beam is nonlinear, and that ambient mechanical vibrations can be modelled as a white Gaussian noise. As a result, the governing equations for the energy harvester form a system of nonlinear stochastic differential equations. In general, the system cannot be solved analytically, and numerical solution, although feasible, require lengthy simulations, especially when a large parameter space must be explored.

We use a power series method to obtain an analytical, although approximate, solution, that can be used to optimize the matching network.

We show that application of the optimized matching network improves the power transferred to the load, and the power efficiency of about 9 times, with respect to the resistive load even in the case of the full SDE model solution

References

1. Penella-Lòpez, M.T., Gasulla-Forner, M.: Powering Autonomous Sensors An Integral Approach with Focus on Solar and RF Energy Harvesting. Springer London, Limited (2011)
2. Roundy, S., Wright, P.K., Rabaey, J.M.: Energy scavenging for wireless sensor networks. Springer (2003)
3. Paradiso, J.A., Starner, T.: Energy scavenging for mobile and wireless electronics. IEEE Pervasive Computing 4(1), 18–27 (2005).
4. Beeby, S.P., Tudor, M.J., White, N.M.: Energy harvesting vibration sources for microsystems applications. Measurement Science and Technology 17(12), R175 (2006).
5. Mitcheson, P., Yeatman, E., Rao, G., Holmes, A., Green, T.: Energy harvesting from human and machine motion for wireless electronic devices. Proceedings of the IEEE 96(9), 1457–1486 (2008).
6. Lu, X., Wang, P., Niyato, D., Kim, D.I., Han, Z.: Wireless networks with RF energy harvesting: A contemporary survey. IEEE Communications Surveys & Tutorials 17(2), 757–789 (2015).
7. Akinaga, H.: Recent advances and future prospects in energy harvesting technologies. Japanese Journal of Applied Physics 59(11), 110,201 (2020).
8. Bonnin, M., Traversa, F.L., Bonani, F.: Leveraging circuit theory and nonlinear dynamics for the efficiency improvement of energy harvesting. Nonlinear Dynamics 104(1), 367–382 (2021).
9. Huang, D., Zhou, S., Litak, G.: Analytical analysis of the vibrational tristable energy harvester with a RL resonant circuit. Nonlinear Dynamics 97(1), 663–677 (2019).
10. Bonnin, M., Traversa, F.L., Bonani, F.: An impedance matching solution to increase the harvested power and efficiency of nonlinear piezoelectric energy harvesters. Energies 15(8), 2764 (2022).
11. Gardiner, C.W., et al.: Handbook of stochastic methods, vol. 3. Springer Berlin (1985)
12. Øksendal, B.: Stochastic Differential Equations, 6th edn. Springer–Verlag, Berlin (2003)
13. Bonnin, M., Song, K.: Frequency domain analysis of a piezoelectric energy harvester with impedance matching network. Energy Harvesting and Systems 100(1), 119–133 (2022).
14. Bonnin, M., Song, K., Traversa, F.L., Bonani, F.: A Circuit Theory Perspective on the Modeling and Analysis of Vibration Energy Harvesting Systems: A Review. Computation 11(3), 45 (2023)